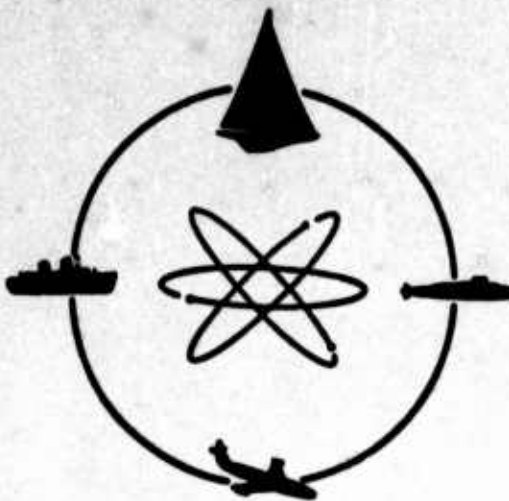


AD645069



DAVIDSON LABORATORY

REPORT 1192

DDC
RECEIVED
JAN 16 1967
R
D

STEVENS INSTITUTE
OF TECHNOLOGY
CASTLE POINT STATION
HOBOKEN, NEW JERSEY

EXPERIMENTAL STUDY OF SPRAY DRAG
OF SOME VERTICAL SURFACE-PIERCING STRUTS

by

Daniel Savitsky and John P. Breslin

December 1966

Distribution of this document is unlimited.

DAVIDSON LABORATORY

REPORT 1192

December 1966

EXPERIMENTAL STUDY OF SPRAY DRAG
OF SOME VERTICAL SURFACE-PIERCING STRUTS

by

Daniel Savitsky and John P. Breslin

Sponsored by
Office of Naval Research
Administered by David Taylor Model Basin
Contract Nonr 263(34); EN24/314-15-60
(DL Project LI-2272)

Distribution of this document is unlimited. Application for copies may be made to the Defense Documentation Center, Cameron Station, 5010 Duke Street, Alexandria, Virginia 22314. Reproduction of the document in whole or in part is permitted for any purpose of the United States Government.

iii + 17 pages
4 tables, 4 figures

ABSTRACT

→ Experimental results obtained at high Froude number for a series of NACA 4 digit airfoil section surface-piercing struts show that the spray drag is essentially independent of operating Froude number and strut leading edge radius. The spray drag increases with strut thickness ratio and can be as much as 40% of the strut profile drag for typical operating conditions. () ↗

Keywords

Surface Piercing Strut

Spray Drag

Hydrofoils

TABLE OF CONTENTS

ABSTRACT	iii
NOMENCLATURE	vii
INTRODUCTION	1
MODELS AND INSTRUMENTATION	2
Models	2
Test Set-Up and Instrumentation	2
METHOD FOR ANALYZING THE DRAG DATA	4
Residual Drag	5
Added Drag of Lower Tip	6
RESULTS AND DISCUSSION	7
Profile Drag Coefficient (C_{D_p})	7
Spray Drag Coefficient (C_{D_s})	8
Effect of Froude Number on C_{D_s}	9
Effect of Strut Leading Edge Radius on C_{D_s}	9
Effect of Strut Thickness Ratio on C_{D_s}	10
CONCLUSIONS	12
REFERENCES	12
TABLES	13
FIGURES 1-4	

NOMENCLATURE

- D_T total drag, lb.
- D_P profile drag, lb.
- D_O residual drag = extrapolated drag for zero depth, (spray drag plus submerged tip drag), lb.
- D_t tip drag, lb.
- D_s spray drag, ($D_O - D_t$), lb.
- C_D total drag coefficient, $\frac{D_T}{\rho/2 V^2 c^2}$
- C_{D_P} profile drag coefficient, $\frac{D_P}{\rho/2 V^2 cd}$
- C_{D_O} residual drag coefficient, $\frac{D_O}{\rho/2 V^2 c^2}$
- C_{D_t} tip drag coefficient, $\frac{D_t}{\rho/2 V^2 c^2}$
- $C_{D_{s_o}}$ spray drag coefficient = $C_{D_O} - C_{D_t}$
- C_{D_s} spray drag coefficient, $\frac{D_s}{\rho/2 V^2 ct}$
- c strut chord, ft.
- d depth of submergence from the undisturbed water surface to the lower end of the prismatic section of the foil (excluding the faired tip), ft.
- t maximum thickness of strut, ft.
- V speed, fps

- q dynamic pressure = $\frac{\rho}{2} v^2$, lb/sq.ft.
- FN Froude number $\frac{v}{\sqrt{gc}}$
- RN Reynolds number, $\frac{vc}{\nu}$
- g gravitational acceleration, ft/sec²
- ρ mass density of water, slugs/cu.ft.
- γ kinematic viscosity of water, ft²/sec.
- AR aspect ratio, d/c
- LER leading edge radius

INTRODUCTION

This report is concerned with a study of the free surface effect on the drag of some vertical surface-piercing struts having symmetrical sections and moving at zero angle of attack and at constant speed. This drag component is usually referred to as the "spray drag" although it is more properly descriptive of the free-surface drag. Data of this type are of interest in the design of hydrofoil craft and, at times, in the design and operation of hydrodynamic model test facilities where surface-piercing struts are employed as part of the experimental rig.

The emphasis of the present study was to explore the effect of strut thickness and leading edge radius on the spray drag component. Five NACA 4 digit symmetrical airfoil sections were used in this study -- all were tested at zero angle of attack.

The work was sponsored by the Office of Naval Research and Administered by the David Taylor Model Basin under Contract Nonr 263(34); EN 24/314-15-60.

MODELS AND INSTRUMENTATION

Models:

Five strut models with NACA 4 digit cross sections were constructed of mild steel, polished to a close tolerance. The models have sizes and properties shown in the sketch and Table I below. The lower tip of each model was half of a body of revolution formed by rotating a half section about the axis of symmetry. As the NACA designations listed in Table I indicate, all models have the position of maximum thickness at the 3/10 point from the leading edge.

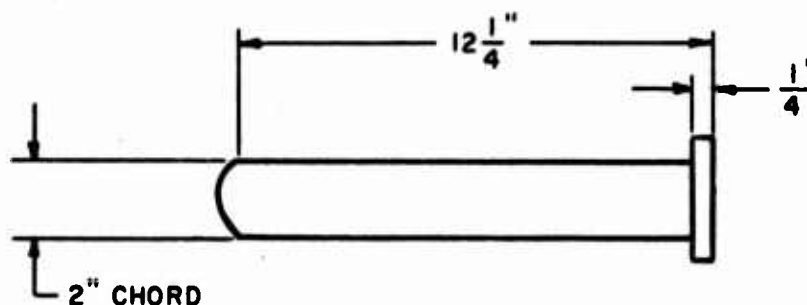


Table I

Model	"A"	"B"	"C"	"D"	"E"
NACA designation	0010-63	0020-33	0020-63	0020-93	0030-63
Thickness/Chord	.10	.20	.20	.20	.30
(Leading edge radius)/Chord	.0110	.0109	.0439	.1322	.0990

Note: "B" and "D" are sections having leading edge radii smaller and larger respectively than the standard section "C" of the same thickness.

Test Set-Up and Instrumentation:

All tests were conducted in Tank No. 3 of the Davidson Laboratory. This test facility is 313 ft. long, 12 ft. wide, and nominally 6 ft. deep. The test models were rigidly attached at their upper end to the standard DL-10 lb. drag balance which was located above the water surface and attached

to the towing carriage. The test set-up was designed to provide for rapid adjustment of the wetted length of the surface-piercing strut. All tests were made with the strut at zero angle of attack which was achieved by aligning the strut with the towing rail system by means of an optical sighting device. The drag measurements were corrected for air tare obtained by running the carriage at different speeds with the lower tip of the model set just above the level water surface.

The test models listed in Table I were towed vertically at zero angle of attack and at the following test conditions.

Test speed; fps:	10	20	30
Chord Reynolds No.	1.36×10^5	2.72×10^5	4.06×10^5
Chord Froude No.	4.33	8.66	13.00
Submergence Depths:	1 to 5 Chords		
Submerged Aspect Ratio:	1 to 5		

In all cases the total drag force and the strut tip submergence below the static water line were measured. No attempt was made to artificially induce a turbulent flow over the foil section since successive test runs were made at a three-minute cycle in order to maintain a high level of residual turbulence in the towing tank.

METHOD FOR ANALYZING THE DRAG DATA

The drag force acting on any body moving rectilinearly at constant speed through a fluid is basically considered as the integrated effect of those components of the shear and pressure forces which act parallel to the direction of motion. The sum of the shear force and the so-called viscous pressure drag is termed the profile or section drag in two-dimensional flows. For surface-piercing struts, about which there are three-dimensional flows, the section drag is not the same for each section because of the presence of the free surface and because of the flows about the submerged tip of the strut. The presence of the free surface is evidenced in the following three ways:

1. The pressure along the free surface intersection with the strut must be constant atmospheric. This implies that the pressure drag for sections near the free surface must be less than the section drag for deeply submerged sections.
2. Formation of surface waves and attendant wave drag. The wave drag component is of importance at low Froude number and is negligible at very high values of Froude number.
3. Formation of spray and attendant spray drag. This drag component is of importance only at the higher Froude numbers.

The drag attributed to the three-dimensional nature of the flows about the submerged end of the strut is entirely dependent upon the geometric conditions of the lower end; i.e., whether the lower end of the strut is connected to a hydrofoil, a nacelle, or if it is a free end, etc. It is not the intent of the present study to investigate, in any detail, the drag influence of the lower tip. Consideration will, however, be given to estimating the lower tip drag of the particular test models studied in this investigation.

Residual Drag:

The intent of the present study is to isolate the effect of the free surface on the total drag of several surface-piercing struts at very high Froude numbers ($FN > 4.3$) wherein it can be assumed that the wave drag component is negligible. This can be accomplished if the tests and subsequent data analysis are conducted in the following manner.

The total measured resistance (less air tares) will be plotted in the form $D_T/q(c)^2$ as a function of submergence, d , for a strut (chord = c) towed at constant speed ($FN > 4.3$), and at zero angle of attack for several submergences greater than at least one chord. If these conditions are fulfilled, the variation of total drag with submergence will be linear and the slope of the line through these data will be the two-dimensional profile drag. Furthermore, the intercept at $d = 0$ will be the sum of the free surface contribution to profile drag and the lower tip drag.

In terms of the given nomenclature, the total drag is:

$$D_T = D_p + D_o \quad (1)$$

where:

D_T = total drag

D_p = profile drag (two-dimensional)

D_o = residual drag (free surface effect plus submerged tip drag)

dividing each term by qc^2

$$\frac{D_T}{qc^2} = \frac{D_p}{qcd} \cdot \frac{d}{c} + \frac{D_o}{qc^2} \quad (2)$$

from the definitions given in the notation page:

$$C_D = C_{D_p} \cdot \frac{d}{c} + C_{D_o} \quad (3)$$

For a given value of C_{D_o} , this is a linear equation expressing the relation between C_D and d/c . Rewriting equations (2) and (3):

$$D_T = \left[C_{D_p} qcd \right] + D_o \quad (4)$$

where C_{D_p} , the two-dimensional profile drag coefficient, is assumed constant. Then at $d = 0$, the drag $D_T = D_o$, (free surface effect plus submerged tip drag).

Added Drag of Lower Tip:

The lower tip of each of the tested NACA four-digit series struts was a rounded half-body of revolution found by rotating a half section about the longitudinal axis of symmetry. Using an empirical formulation derived by S.F. Hoerner¹ it is seen that the drag of a wing tip with rounded edges is "negative". This means that the total parasitic drag of the wing with a rounded tip is lower than the two-dimensional section drag -- evidently because of the three-dimensional flow conditions about the tips. For a single wing tip with a "rounded" edge, Hoerner estimates the tip drag to be:

$$C_{D_t} = -.02\left(\frac{t}{c}\right)^2 \quad \text{for } \left(\frac{t}{c}\right) < 0.30 \quad (5)$$

No attempt has been made in this study to verify equation (5).

RESULTS AND DISCUSSION

All the test data, corrected for aerodynamic tare, are given in Table II in the form of total hydrodynamic drag, D_T , and total hydrodynamic drag coefficient, C_D . The drag coefficients for the 20% thick struts, (Models B, C, and D), are plotted in Figure 1 as a function of submergence aspect ratio. Separate plots are given for each leading edge radius and on each plot the hydrodynamic data are presented for each of the three test speeds. Figure 2 presents similar data plots for the standard NACA four-digit airfoils having thickness ratios of 10%, 20% and 30% (Models A, C, and E).

It is seen, in Figures 2 and 3, that the data for each test speed are very well fitted by a straight line relation such as suggested by Equation (3). Hence the method of data analysis proposed in the previous section of this report has been utilized to separate and define the various drag components of the surface-piercing struts. The slope of the straight lines for each test speed has been evaluated to determine the profile drag coefficient, C_{D_p} . The zero draft intersect has been obtained by extrapolating the straight lines for d/c values less than 1.0 to obtain the residual drag coefficient C_{D_0} . These drag components are presented in Table III for each test model and each test speed. The estimate of the lower tip drag given Equation (5) is also tabulated and subtracted from the residual drag coefficients to obtain the so-called "spray drag" coefficient $C_{D_{s_0}}$.

An analysis of these tabulated data is given below for the profile drag coefficient and spray coefficient.

Profile Drag Coefficient (C_{D_p}):

The profile drag coefficients given in Table III are plotted in Figure 3 as a function of thickness ratio for each test Reynolds number. For comparative purposes, profile drag coefficients obtained by NACA for a 4-digit airfoil series (Ref. 2) are also presented on Figure 3. These NACA data were obtained at a test Reynolds number of 6×10^6 -- nearly an order

of magnitude higher than the maximum test Reynolds number in the Davidson Laboratory tests.

The leading edge radius was found to have only a small effect on the profile drag coefficient so that, for Models B, C, E -- all having a $t/c = 0.20$, an average value of C_{D_p} is taken for each test speed. Hence Figure 3 shows separate curves demonstrating the variation of C_{D_p} versus t/c for each test Reynolds number. It is seen that, at each test Reynolds number, the profile drag coefficient increases approximately linearly with increasing thickness ratio -- an effect which is consistent with the aerodynamic results of Ref. 2.

As expected, it is seen that the drag coefficient decreases with increasing Reynolds number. The high drag at low Reynolds numbers is caused principally by a relatively extensive region of laminar separation downstream from the point of minimum pressure. This region decreases in size with increasing Reynolds number and with increasing ambient turbulence level which influences the extent of the laminar boundary layer.

No further analysis of these limited profile drag data will be made in this report except to state that the general trends in variation of drag with t/c and RN shown in Figure 3 are in agreement with aerodynamic test data (Ref. 2). For practical design applications it is recommended that the profile drag coefficients obtained at high Reynolds numbers ($RN > 6 \times 10^6$) be used (Ref. 2).

Spray Drag Coefficient (C_{D_s}):

The residual drag coefficients, C_{D_o} , obtained from the extrapolated zero draft intercepts in Figures 1 and 2 are given in Table III. It will be recalled that the residual drag represents the sum of the free surface spray drag and lower tip drag. It is seen that, for each test model, the residual drag is essentially independent of Reynolds number for the range of speeds considered in this study. The small variations in C_{D_o} that do appear for each model are well within the accuracy of the linear extrapolation of data shown in Figures 1 and 2.

The estimated lower tip drag, C_{D_t} , given by Equation (5) is also given in Table III. This drag component is, in accordance with Ref. 1,

independent of Reynolds number and hence is a constant for each test model. Because the lower tip of the test strut is rounded the drag correction is negative, i.e., causes a reduction in the profile drag. On the average, the tip drag is approximately 10% of the residual drag for all test models. This lower tip drag is subtracted from the residual drag to obtain the free-surface spray drag coefficient, $C_{D_{s_0}}$, which is also presented in Table III.

In analyzing the spray drag it was considered to be more meaningful if the coefficient of spray drag was defined as $C_{D_s} = D_s/qct$ rather than as $C_{D_{s_0}} = D_s/qc^2$ given in Table III. This is because the spray drag is expected to be dependent upon both the chord, c , which is representative of the extent of the strut surface wetted by the spray and the thickness, t , which governs the pressure distribution on the strut. Accordingly, this C_{D_s} definition of spray drag has been evaluated and is given in Table IV.

Effect of Froude Number on C_{D_s} : An examination of the tabulated values of C_{D_s} for each strut model shows that, for the present high Froude number test conditions, wherein the gravity or wave making effects are small, there is little variation in C_{D_s} with Froude or Reynolds number. As in the case of the residual drag, the small variation in C_{D_s} that do appear for each test strut are well within the accuracy of the extrapolation of data shown in Figures 1 and 2. Hence it is concluded that, for the NACA 4-digit airfoil sections, the spray drag coefficient is independent of Froude number for $FN > 4.3$.

Effect of Strut Leading Edge Radius on C_{D_s} : Models B, D, and C were struts having a thickness ratio of 20% and LER/c values of 0.0109; 0.0132; and 0.0439 respectively. An examination of the tabulated values of C_{D_s} for these strut models does not show any consistent variation in spray drag coefficient with leading edge radius. The strut having the largest value of LER/c (Model C) has values of C_{D_s} intermediate to those of Models B and D -- both struts having smaller values of leading edge radius than strut C. The difference between the average C_{D_s} values for these three strut models is, however, very small so that, for practical engineering design application, it will be assumed that the spray drag is independent of leading edge

radius. This conclusion must, of course, be limited to the range of LER/c values considered in the present study.

Effect of Strut Thickness Ratio on C_{D_s} : Figure 4 presents a plot of spray drag coefficient versus t/c for all test models. No attempt has been made to prepare separate curves for each RN or LER/c since, in accordance with the previous discussions the effect of RN and LER/c are found to be very small.

It is seen in Figure 4 that the experimental data can be represented by a linear relation between C_{D_s} and t/c . The empirical equation expressing this relation is found to be:

$$C_{D_s} = .03 + .08 \frac{t}{c} \quad (6)$$

This relationship is, of course, limited to ranges of t/c between .10 and .30 for the NACA 4-digit airfoil series.

The thickness ratio is thus found to have a significant effect on the spray drag of surface-piercing struts. Using Equation (6), the spray drag is:

$$D_s = [.03tc + .08t^2]q \quad (7)$$

Hence, for a given chord dimension, c , the spray drag increases in a combined linear and quadratic function of strut thickness t .

This brief series of experiments have shown that the spray drag is indeed an important contribution to the total drag of surface-piercing struts. For instance, if a submergence aspect ratio of 2.0 is taken as a typical strut operating condition; a strut thickness ratio of 10% is assumed, then for the largest test Reynolds number considered in these tests, (4.06×10^5) the spray drag will be approximately 40% of the strut profile drag. This percentage will increase for increasing Reynolds numbers since the strut profile drag coefficient decreases with Reynolds number while the spray drag coefficient has been shown to be essentially independent of Reynolds number. With increasing strut thickness ratio the spray drag contribution to total strut drag is even more substantial. For instance,

for a $t/c = 30\%$, all other conditions being the same as for the $t/c = 10\%$ case, the spray drag will be increased to nearly 60% of the strut profile drag.

It would be of great interest if additional data could be obtained for other strut sections and higher values of Reynolds number in order to ascertain the adequacy of applicability of Equation (6) over wider practical operating conditions.

CONCLUSIONS

Experiments have been conducted to evaluate the spray drag associated with NACA 4-digit airfoil section surface-piercing struts operating at Froude numbers greater than 4.0; Reynolds numbers less than 4.06×10^5 ; submergence aspect ratios between 1 and 5; and strut thickness ratios between 10% and 20%. The following effects were found:

1. The spray drag coefficient was essentially independent of Reynolds number or Froude number.
2. The leading edge radius had a small effect on the magnitude of the spray drag.
3. Thickness ratio had a most pronounced effect on spray drag coefficient and is defined by the following empirical relation.

$$C_{D_s} = \frac{D_s}{qct} = .03 + .08 \frac{t}{c}$$

4. For typical operating conditions of surface-piercing struts, the spray drag can be as high as 40% of the strut profile drag.

REFERENCES

1. Hoerner, S.F. "Fluid-Dynamic Drag", Published by the Author, 1958.
2. Abbott, Ira H. and Von Doenhoff, A.E. "Theory of Wing Sections", Dover Publications, Inc., New York, 1959.

TABLE II

TEST DATA

HYDRODYNAMIC DRAG - SYMMETRICAL SURFACE-PIERCING STRUTS

$$C_d = D_T / \frac{1}{2} \rho V^2 c^2 \quad c = 2.0 \text{ in.}$$

<u>Model A</u>				<u>Model B</u>			
t/c = 0.10		LER/c = .0110		t/c = 0.20		LER/c = .0109	
V	d	D _T	C _D	V	d	D _T	C _D
10.20 fps	2.0 in.	.045 lb.	.0155	10.20 fps	2.0 in.	.069 lb.	.024
	3.0	.054	.019		3.0	.089	.031
	4.0	.067	.023		4.0	.112	.039
	6.0	.100	.034		6.0	.157	.054
	8.0	.131	.045		8.0	.196	.068
	10.0	.156	.054	10.0	.241	.083	
20.16	2.0	.122	.011	20.16	2.0	.207	.018
	3.0	.157	.014		3.0	.280	.025
	4.0	.201	.018		4.0	.324	.029
	6.0	.291	.026		6.0	.451	.040
	8.0	.362	.032		8.0	.574	.051
	10.0	.456	.040	10.0	.705	.063	
30.30	2.0	.233	.009	30.30	2.0	.431	.017
	3.0	.315	.012		3.0	.563	.022
	4.0	.413	.016		4.0	.661	.026
	6.0	.560	.022		6.0	.906	.035
	8.0	.721	.028		8.0	1.155	.045
	10.0	.903	.035	10.0	1.417	.055	

TABLE II (continued)

TEST DATA

HYDRODYNAMIC DRAG - SYMMETRICAL SURFACE-PIERCING STRUTS

$$C_d = D_T / \frac{1}{2} \rho V^2 c^2 \quad c = 2.0 \text{ in.}$$

<u>Model C</u>				<u>Model D</u>			
t/c = 0.20		LER/c = 0.0439		t/c = 0.20		LER/c = 0.01322	
V	d	D _T	C _D	V	d	D _T	C _D
10.20 fps	2.0 in.	.073 lb.	.025	10.20 fps	2.0 in.	.079 lb.	.028
	3.0	.094	.032		3.0	.102	.035
	4.0	.117	.040		4.0	.126	.044
	6.0	.160	.055		6.0	.163	.056
	8.0	.205	.071		8.0	.212	.073
	10.0	.244	.084		10.0	.255	.088
20.20	2.0	.227	.020	20.16	2.0	.257	.0227
	3.0	.305	.027		3.0	.325	.0287
	4.0	.369	.033		4.0	.379	.0334
	6.0	.500	.044		6.0	.526	.0465
	8.0	.627	.056		8.0	.653	.0576
	10.0	.753	.067		10.0	.813	.0716
30.30	2.0	.505	.0197	30.30	2.0	.517	.020
	4.0	.801	.0313		4.0	.784	.031
	6.0	1.056	.0413		6.0	1.049	.041
	8.0	1.355	.0530		8.0	1.338	.052
	10.0	1.591	.0623		10.0	1.613	.063

TABLE II (continued)

TEST DATA

HYDRODYNAMIC DRAG - SYMMETRICAL SURFACE-PIERCING STRUTS

$$C_d = D_T / \frac{1}{2} \rho V^2 c^2 \quad c = 2.0 \text{ in.}$$

Model E

t/c = 0.30 LER/c = 0.0990

V	d	D _T	C _D
10.20 fps	2.0 in.	.109 lb.	.038
	3.0	.134	.046
	4.0	.172	.059
	6.0	.233	.081
	8.0	.296	.103
	10.0	.361	.126
20.16	2.0	.337	.030
	3.0	.445	.039
	4.0	.509	.045
	6.0	.666	.059
	8.0	.848	.075
	10.0	1.113	.100
30.30	2.0	.689	.027
	4.0	1.030	.040
	6.0	1.333	.052
	8.0	1.688	.066
	10.0	2.247	.084

TABLE III
DRAG COMPONENTS - SYMMETRICAL SURFACE-PIERCING STRUTS

Model	t/c	LER/c	RN	C_{D_o}	C_{D_p}	C_{D_t}	$C_{D_{s_o}}$
A	0.10	0.0110	4.06×10^5	.0030	.0063	-.0002	.0032
			2.72	.0035	.0073	-.0002	.0037
			1.36	.0040	.0100	-.0002	.0042
B	0.20	0.0109	4.06×10^5	.0080	.0094	-.0008	.0088
			2.72	.0080	.0109	-.0008	.0088
			1.36	.0080	.0150	-.0008	.0088
C	0.20	0.0439	4.06×10^5	.0085	.0109	-.0008	.0093
			2.72	.0090	.0116	-.0008	.0098
			1.36	.0095	.0149	-.0008	.0103
D	0.20	0.0132	4.06×10^5	.0090	.0108	-.0008	.0098
			2.72	.0100	.0123	-.0008	.0108
			1.36	.0120	.0152	-.0008	.0128
E	0.30	0.0990	4.06×10^5	.0150	.0127	-.0018	.0168
			2.72	.0150	.0142	-.0018	.0168
			1.36	.0150	.0219	-.0018	.0168

$$C_{D_o} = \text{Residual Drag Coefficient} = \frac{D_o}{\frac{\rho}{2} V_c^2 c^2}$$

$$C_{D_p} = \text{Profile Drag Coefficient} = \frac{D_p}{\frac{\rho}{2} V_c^2 c d}$$

$$C_{D_t} = \text{Estimated Tip Drag Coefficient} = \frac{D_t}{\frac{\rho}{2} V_c^2 c^2}$$

$$C_{D_{s_o}} = \text{Free Surface Drag Coefficient} = \frac{D_s}{\frac{\rho}{2} V_c^2 c^2} = C_{D_o} - C_{D_t}$$

TABLE IV

SPRAY DRAG - SYMMETRICAL SURFACE-PIERCING STRUTS

$$C_{D_{s_0}} = \frac{D_s}{q V^2 c^2}$$

$$C_{D_s} = C_{D_{s_0}} \cdot \frac{c}{t} = \frac{D_s}{q V^2 c t}$$

Model	t/c	LER/c	RN	$C_{D_{s_0}}$	C_{D_s}
A	.10	0.0110	4.06×10^5	.0032	.032
			2.72	.0037	.037
			1.36	.0042	.042
B	.20	0.0109	4.06×10^5	.0088	.044
			2.72	.0088	.044
			1.36	.0088	.044
C	.20	0.0439	4.06×10^5	.0093	.046
			2.72	.0098	.049
			1.36	.0103	.051
D	.20	0.0132	4.06×10^5	.0098	.049
			2.72	.0108	.054
			1.36	.0128	.064
E	.30	0.0990	4.06×10^5	.0168	.056
			2.72	.0168	.056
			1.36	.0168	.056

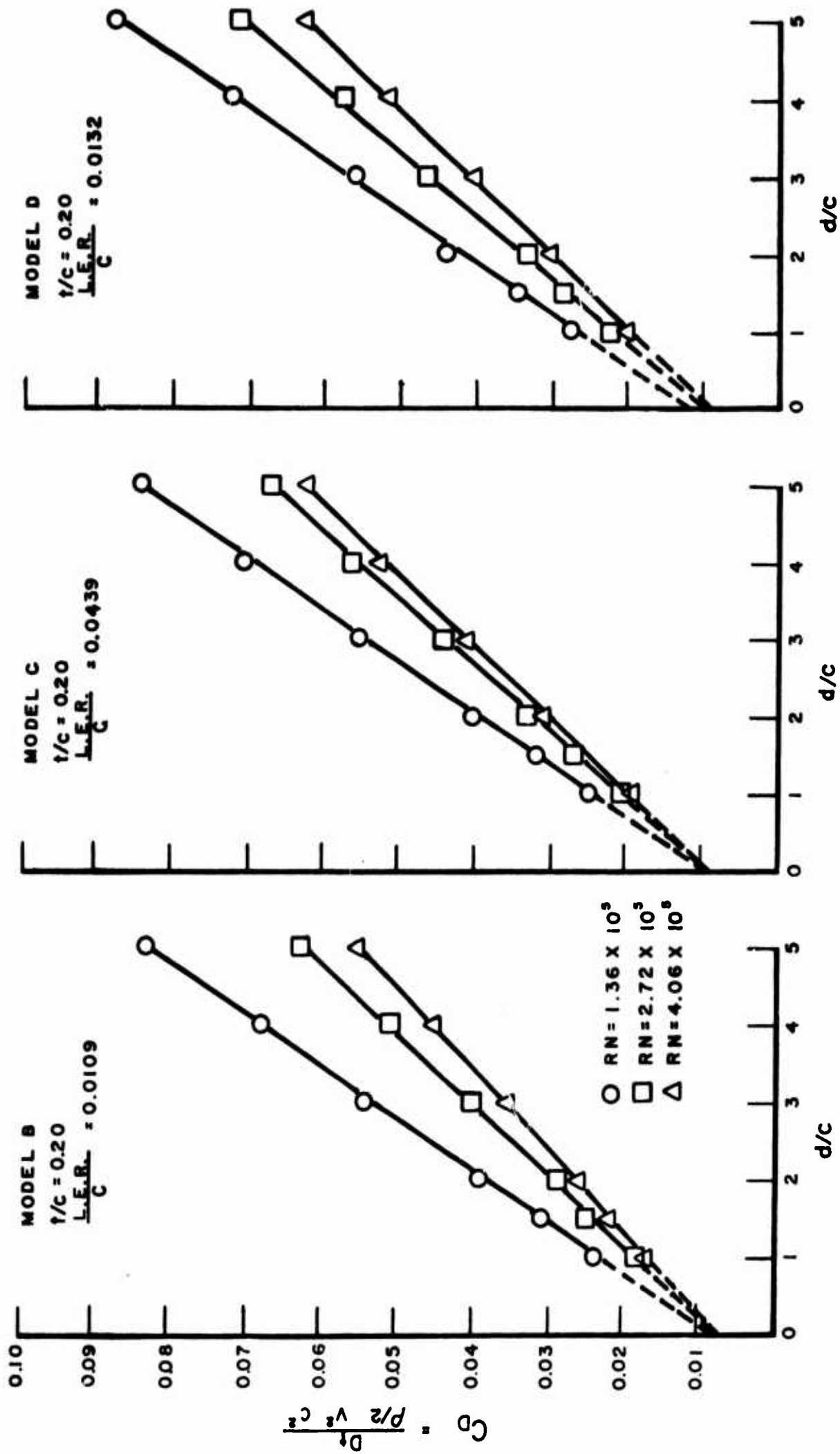


FIGURE 1. VARIATION OF TOTAL DRAG WITH SUBMERGENCE $t/c = 0.20$ VARYING L.E.RADIUS

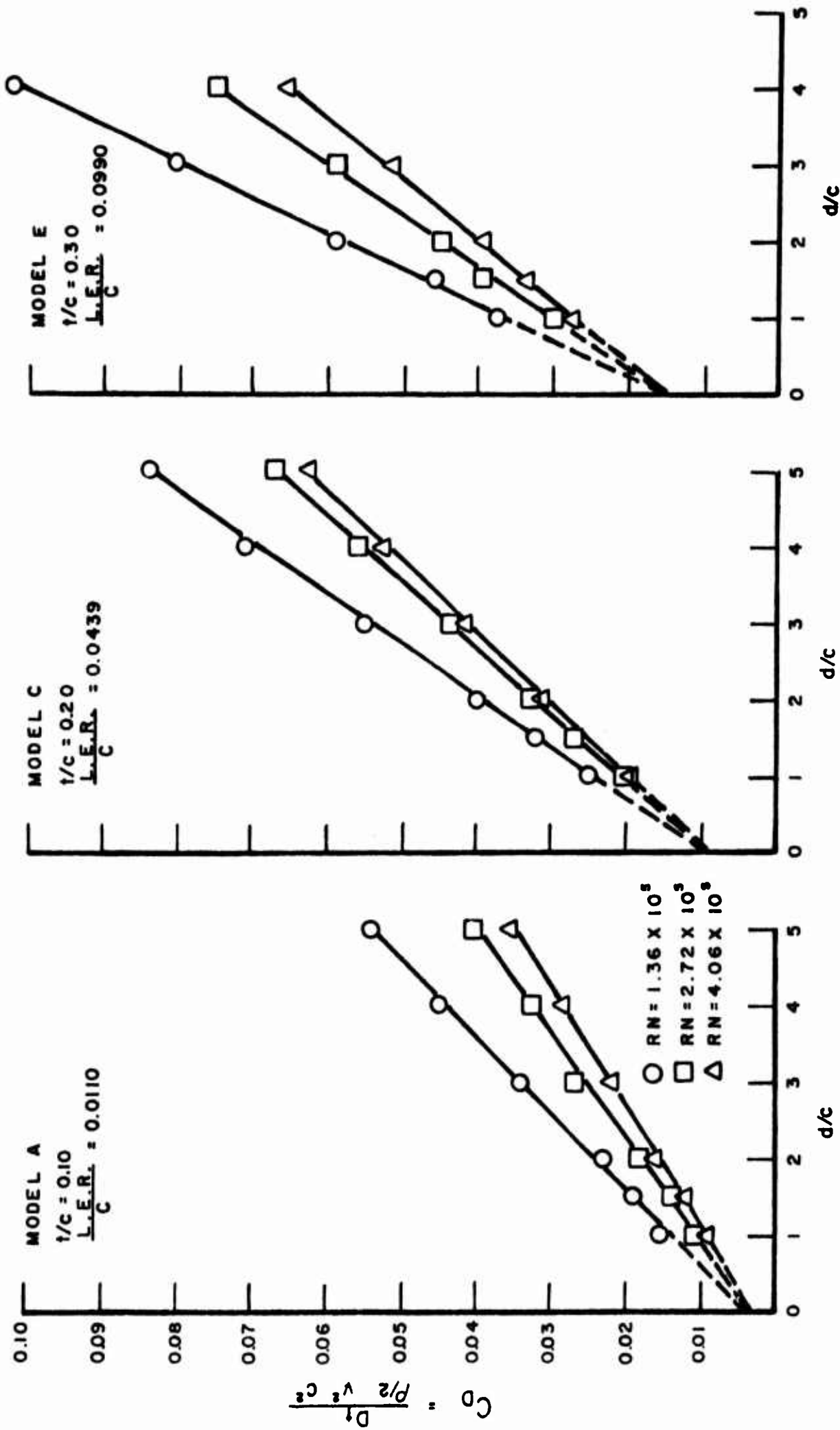


FIGURE 2. VARIATION OF TOTAL DRAG WITH SUBMERGENCE AND THICKNESS RATIO

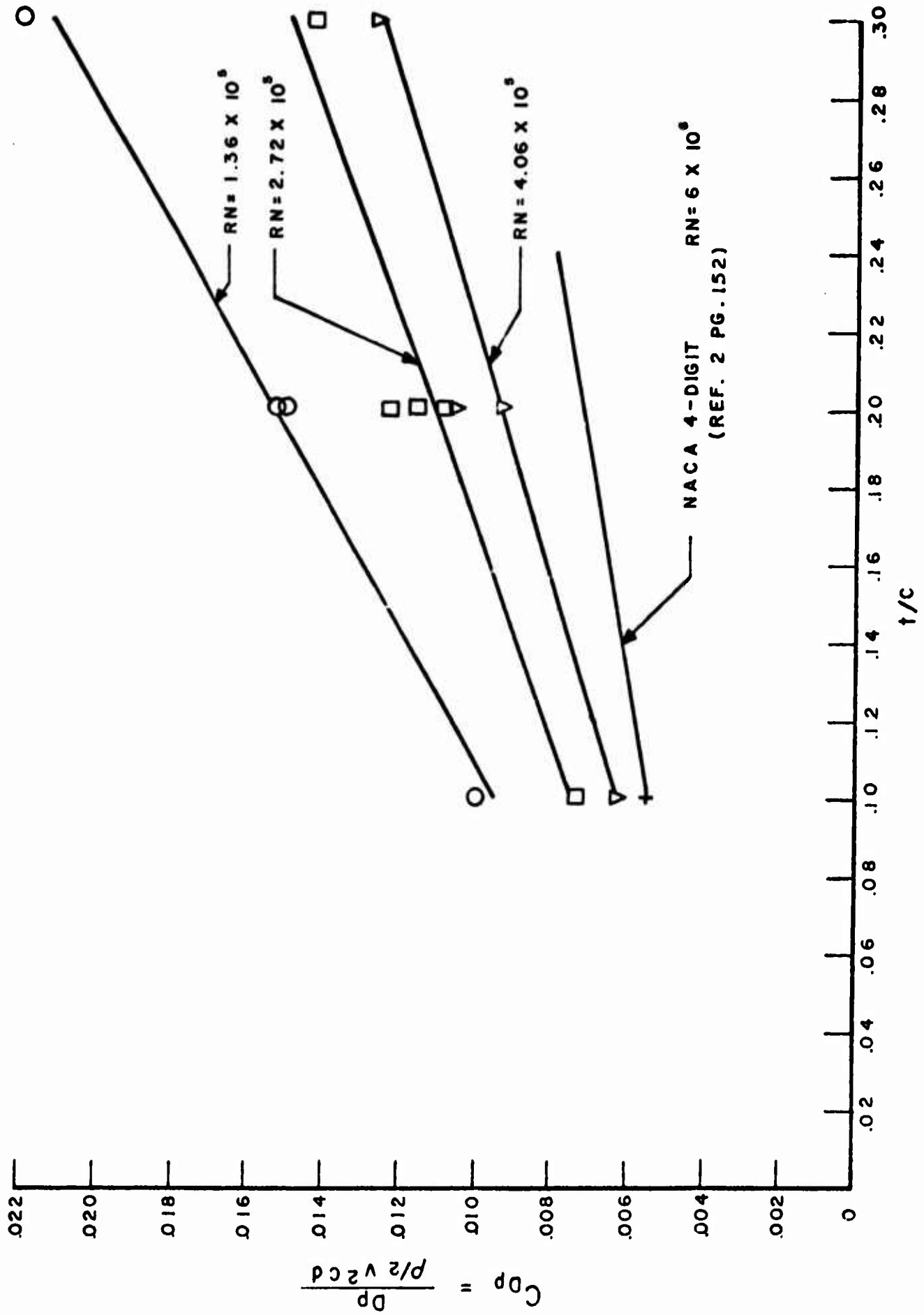


FIGURE 3. VARIATION OF PROFILE DRAG WITH t/c

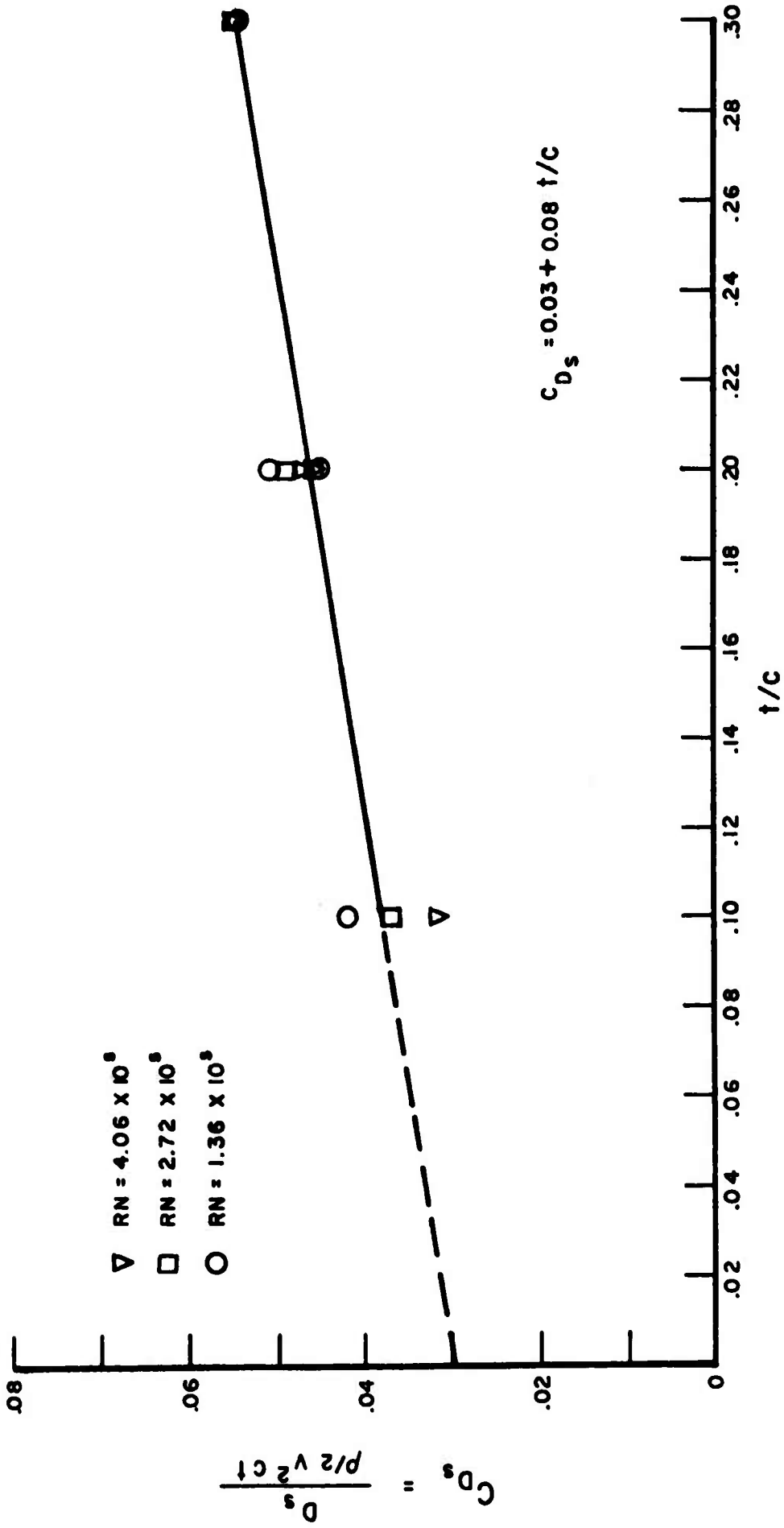


FIGURE 4. VARIATION OF SPRAY DRAG WITH t/c

DOCUMENT CONTROL DATA - R&D

(Security classification of title, body of abstract and indexing annotation must be entered when the overall report is classified)

1. ORIGINATING ACTIVITY (Corporate author) Davidson Laboratory Stevens Institute of Technology		2a. REPORT SECURITY CLASSIFICATION Unclassified	
2b. GROUP			
3. REPORT TITLE EXPERIMENTAL STUDY OF SPRAY DRAG OF SOME VERTICAL SURFACE-PIERCING STRUTS			
4. DESCRIPTIVE NOTES (Type of report and inclusive dates) Final			
5. AUTHOR(S) (Last name, first name, initial) Savitsky, Daniel and Breslin, John P.			
6. REPORT DATE December 1966		7a. TOTAL NO. OF PAGES 17 + 4 figures	7b. NO. OF REFS 2
8a. CONTRACT OR GRANT NO. Nonr 263(34); EN24/314-15-60		9a. ORIGINATOR'S REPORT NUMBER(S) R-1192	
b. PROJECT NO.		9b. OTHER REPORT NO(S) (Any other numbers that may be assigned this report)	
c.			
d.			
10. AVAILABILITY/LIMITATION NOTICES Qualified requesters may obtain copies of this report from DDC.			
11. SUPPLEMENTARY NOTES		12. SPONSORING MILITARY ACTIVITY Office of Naval Research, Washington, D. C. David Taylor Model Basin, Washington, D. C.	
13. ABSTRACT Experimental results obtained at high Froude number for a series of NACA 4 digit airfoil section surface-piercing struts show that the spray drag is essentially independent of operating Froude number and strut leading edge radius. The spray drag increases with strut thickness ratio and can be as much as 40% of the strut profile drag for typical operating conditions.			

14. KEY WORDS	LINK A		LINK B		LINK C	
	ROLE	WT	ROLE	WT	ROLE	WT
<p align="center">Surface Piercing Strut Spray Drag Hydrofoils</p>						

INSTRUCTIONS

1. ORIGINATING ACTIVITY: Enter the name and address of the contractor, subcontractor, grantee, Department of Defense activity or other organization (*corporate author*) issuing the report.

2a. REPORT SECURITY CLASSIFICATION: Enter the overall security classification of the report. Indicate whether "Restricted Data" is included. Marking is to be in accordance with appropriate security regulations.

2b. GROUP: Automatic downgrading is specified in DoD Directive 5200.10 and Armed Forces Industrial Manual. Enter the group number. Also, when applicable, show that optional markings have been used for Group 3 and Group 4 as authorized.

3. REPORT TITLE: Enter the complete report title in all capital letters. Titles in all cases should be unclassified. If a meaningful title cannot be selected without classification, show title classification in all capitals in parenthesis immediately following the title.

4. DESCRIPTIVE NOTES: If appropriate, enter the type of report, e.g., interim, progress, summary, annual, or final. Give the inclusive dates when a specific reporting period is covered.

5. AUTHOR(S): Enter the name(s) of author(s) as shown on or in the report. Enter last name, first name, middle initial. If military, show rank and branch of service. The name of the principal author is an absolute minimum requirement.

6. REPORT DATE: Enter the date of the report as day, month, year; or month, year. If more than one date appears on the report, use date of publication.

7a. TOTAL NUMBER OF PAGES: The total page count should follow normal pagination procedures, i.e., enter the number of pages containing information.

7b. NUMBER OF REFERENCES: Enter the total number of references cited in the report.

8a. CONTRACT OR GRANT NUMBER: If appropriate, enter the applicable number of the contract or grant under which the report was written.

8b, 8c, & 8d. PROJECT NUMBER: Enter the appropriate military department identification, such as project number, subproject number, system numbers, task number, etc.

9a. ORIGINATOR'S REPORT NUMBER(S): Enter the official report number by which the document will be identified and controlled by the originating activity. This number must be unique to this report.

9b. OTHER REPORT NUMBER(S): If the report has been assigned any other report numbers (*either by the originator or by the sponsor*), also enter this number(s).

10. AVAILABILITY/LIMITATION NOTICES: Enter any limitations on further dissemination of the report, other than those

imposed by security classification, using standard statements such as:

- (1) "Qualified requesters may obtain copies of this report from DDC."
- (2) "Foreign announcement and dissemination of this report by DDC is not authorized."
- (3) "U. S. Government agencies may obtain copies of this report directly from DDC. Other qualified DDC users shall request through _____."
- (4) "U. S. military agencies may obtain copies of this report directly from DDC. Other qualified users shall request through _____."
- (5) "All distribution of this report is controlled. Qualified DDC users shall request through _____."

If the report has been furnished to the Office of Technical Services, Department of Commerce, for sale to the public, indicate this fact and enter the price, if known.

11. SUPPLEMENTARY NOTES: Use for additional explanatory notes.

12. SPONSORING MILITARY ACTIVITY: Enter the name of the departmental project office or laboratory sponsoring (*paying for*) the research and development. Include address.

13. ABSTRACT: Enter an abstract giving a brief and factual summary of the document indicative of the report, even though it may also appear elsewhere in the body of the technical report. If additional space is required, a continuation sheet shall be attached.

It is highly desirable that the abstract of classified reports be unclassified. Each paragraph of the abstract shall end with an indication of the military security classification of the information in the paragraph, represented as (TS), (S), (C), or (U).

There is no limitation on the length of the abstract. However, the suggested length is from 150 to 225 words.

14. KEY WORDS: Key words are technically meaningful terms or short phrases that characterize a report and may be used as index entries for cataloging the report. Key words must be selected so that no security classification is required. Identifiers, such as equipment model designation, trade name, military project code name, geographic location, may be used as key words but will be followed by an indication of technical context. The assignment of links, roles, and weights is optional.